IRAMP
15(1), Jan 2024, pp. 1-26

ISSN: 2229-39-44

Review of the Dynamics of Atomic and Molecular Systems of Higher than Geometric Symmetry: Muonic Atoms and Atoms in a High-Frequency Laser Field

N. KRYUKOV*

Universidad Nacional Autónoma de México, Av. Universidad 3000, col. Ciudad Universitaria, del. Coyoacán, México, DF 04510, Mexico
** Corresponding author email: kriukov@gmail.com*

ABSTRACT: In our previous review, we covered various types of one-electron Rydberg quasimolecules in different environments, such as under electric and/or magnetic fields or in plasma. In the present review we cover the dynamics of certain types of muonic atoms with symmetry higher than geometric, as well as the dynamics of various atomic systems subjected to a high-frequency laser field. Examples are hydrogen atoms and hydrogenlike ions, He atoms and He-like ions, Li atoms and Li-like ions. These systems in the high-frequency laser field effectively have the spherical symmetry while their geometrical symmetry is only axial. The review covers various counterintuitive results concerning the dynamics of all of the above atomic systems, as well as their fundamental and practical importance.

Keywords: dynamics of muonic atoms; dynamics of atoms in a high-frequency laser field; higher than geometrical symmetry

TABLE OF CONTENTS

CHAPTER 1. INTRODUCTION

The concept of symmetry plays the crucial role in the dynamics of physical systems. There are two kinds of symmetry. First, there could be a geometrical symmetry dictated by the symmetry of the configuration of the system, for instance, spherical or axial symmetry. Second, there are physical systems possessing a symmetry higher than the geometrical one: the algebraic symmetry. The latter systems are of fundamental importance. The reason is that analytical solutions can be found for such systems due to their algebraic symmetry. This is important because the alternative treatment simulations lack the physical insight provided by the analytical solutions.

In our previous review (referenced in Chapter 2 below) we presented the study of various types of one-electron Rydberg quasimolecules. In the present review, first we cover the dynamics of certain types of muonic atoms with symmetry higher than geometric. Then we review studies of the dynamics of various atomic systems subjected to a high-frequency laser field. Examples are hydrogen atoms and hydrogenlike ions, He atoms and He-like ions, Li atoms and Li-like ions. These systems in the high-frequency laser field effectively have the spherical symmetry while their geometrical symmetry is only axial.

The review covers various counterintuitive results concerning the dynamics of all of the above atomic systems, as well as their fundamental and practical importance. Throughout the whole review, we use atomic units ($\hbar = e = m_e = 1$).

In the first two chapters, we present the studies of muonic atoms, particularly, of muonic-electronic helium and helium-like ions; in the latter one we considered the case of a non-zero eccentricity of the orbits of the subsystem muon – nucleus. The other two chapters contain the studies of helium and lithium atoms or helium/lithium-like ions in a laser field of high frequency.

CHAPTER 2. CLASSICAL ANALYTICAL SOLUTION FOR RYDBERG STATES OF MUONIC-ELECTRONIC HELIUM AND HELIUM-LIKE IONS

2.1. Introduction

In [1,2] we carried out the study of the Rydberg states of the configurations of a nucleus with charge Z, an electron, and also a muon, in the configuration which has both the muon and the electron in circular states – see our previous review [3] (referred below as Part I), specifically Chapter 5 for the case $Z = 1$.[1] We studied such μZe systems (both for $Z = 1$ ([1] and Chapter 5 of [3]) and for $Z > 1$ [2]) considering many practical applications of muonic atoms and molecules, in which one of the electrons is replaced by the heavier particle μ^- (see, e.g., [11-15]). We showed that the muon and electron motion can be considered rapid and slow subsystems accordingly, which at first sight is counterintuitive. In a more illustrative way, the muon rapidly rotates in a circular orbit about the axis connecting the proton and the electron, while this axis slowly rotates together with the relatively slow motion of the electron in a circular orbit. We saw that the spectral lines of the muon in the quasimolecule μpe experience a red shift with respect to the muonic hydrogen spectral lines from the muon.

In this chapter we also study Rydberg states of quasimolecules μZe for $Z > 1$ (i.e, Rydberg states of muonic-electronic helium and helium-like ions) [16]. However, this chapter has differences from [2]. The configurations that we studied here are stable, and the orbit of the electron, in general, is an ellipse (though we neglected the interaction between the electron and the muon). In [2] we took into account the action of the electron on the muon; however, in the rotating frame used in [2] the muon motion is metastable[2]; besides, we only studied circular electronic orbits in [2].

Because the muon motion has a much higher frequency than the electron motion in this muonic type of helium atoms, we use the technique of separating rapid and slow subsystems. We show that the motion of the electron in an effective potential in this system is a mathematical analogue of the satellite motion in the potential of an oblate planet (e.g, the oblate Earth).

Using this corresponding example from celestial mechanics, we found that the unperturbed electron orbit undergoes simultaneously two precessions. One is the precession of the orbit of the electron in the orbital plane, and the other is the precession of the plane of the orbit around the axis of symmetry of the muonic orbit. These two types of precession have different frequencies, and we present analytical expressions for both. We note that the shape of the electron orbit is unchanged under these two precessions. This means that the squared angular momentum of the electron is (approximately) conserved, which shows that there is the *hidden symmetry* in the system.

We remind the reader that, e.g., in the motion in the Coulomb field, this hidden symmetry classically manifests itself by the conservation of the Runge–Lenz vector and quantally manifests itself by the appearance of the additional degeneracy in the energy levels – see. e.g., textbooks [17,18]. For a hydrogen-like atom or ion in an electric field which is uniform in space and constant in time, there is a generalized Runge–Lenz vector [19], the projection of

which on the direction of the electric field is conserved. For an electron in the two-Coulomb-center field, there is a super-generalized Runge–Lenz vector [20], the projection of which on the internuclear axis is conserved.

2.2. Analytical results

We study a μZe-system which consists of a nucleus of charge Z, a muon and an electron. Both leptons are in Rydberg states: their corresponding principal quantum numbers $n_\mu >> 1$ and $n_e >> 1$. Due to the large ratio of their masses ($m_\mu/m_e = 206.8$) the muon is much closer to the nucleus than the electron. We consider the muon to be in a circular Rydberg state, so that its angular momentum quantum number has the maximum value $n_\mu - 1$.

The muon – nucleus revolution frequency about their center of mass is

$$\Omega = \frac{m_{\mu r} Z^2 e^4}{n_\mu^3 \hbar^3} \tag{1}$$

Here

$$m_{\mu r} = \frac{m_\mu M_{nucl}}{m_\mu + M_{nucl}} \tag{2}$$

is the reduced mass of the pair "nucleus – muon" and M_{nucl} is the mass of the nucleus. Particularly, for helium ($Z = 2$), $M_{nucl}/m_\mu = 35.28$, which gives the reduced mass $m_{\mu r} = 201.1$ in atomic units ($\hbar = m_e = e = 1$).

$$\omega_K = \frac{m_{er}(Z-1)^2 e^4}{n_e^3 \hbar^3} \tag{3}$$

Here

$$m_{er} = \frac{m_e(m_\mu + M_{nucl})}{m_e + m_\mu + M_{nucl}} \tag{4}$$

is the reduced mass of the pair "nucleus and muon – electron". Particularly, for helium atoms ($Z = 2$), $m_{er} = 0.9999$ in atomic units, which means that for $Z > 1$, for all intents and purposes we can use $m_{er} = 1$.

From (1) and (3) we get the ratio of the two frequencies and see that it is much greater than unity

$$\frac{\Omega}{\omega_K} = \frac{m_{\mu r} Z^2 n_e^3}{m_{er}(Z-1)^2 n_\mu^3} \gg 1 \tag{5}$$

if the following condition is satisfied:

$$\frac{n_\mu}{n_e} \ll \frac{(m_{\mu r} Z^2)^{1/3}}{(m_{er}(Z-1)^2)^{1/3}} \tag{6}$$

For example, for helium atoms, the condition (6) becomes $n_\mu/n_e << 9$ and the ratio of the frequencies (5) becomes

$$\frac{\Omega}{\omega_K} = 804.4\left(\frac{n_\mu}{n_e}\right)^3 \tag{7}$$

For $Z >> 1$, (6) gives $n_\mu/n_e << 6$ and (5) gives

$$\frac{\Omega}{\omega_K} = 206.8\left(\frac{n_\mu}{n_e}\right)^3 \tag{8}$$

Thus, we see that, for instance, at $n_\mu/n_e \sim 1$, the muon revolution frequency is greater than the electron Kepler frequency by 2 – 3 orders of magnitude (of course, Ω/ω_K is even larger for $n_\mu/n_e < 1$). So, the pair "nucleus – muon" indeed represents a rapid subsystem, and the electron represents a slow subsystem.

Therefore, to solve for the electron orbit in the second-order approximation, we perform averaging over the rapid subsystem. This presents the physical situation described below. The electron perceives both the muon and the nucleus as circular rings of radii R_μ and R_{nucl}, respectively, with the charge of each one uniformly distributed over the ring of the corresponding radius (R_μ and R_{nucl}). The ratio of these radii is

$$\frac{R_\mu}{R_{nucl}} = \frac{M_{nucl}}{m_\mu} \gg 1 \tag{9}$$

Particularly, for helium, $R_\mu/R_{nucl} = 35.28$.

Therefore, the motion of the electron occurs in the effective potential energy which includes two terms, $U^{(1)}$ and $U^{(2)}$. The first term $U^{(1)}$ is the effective Coulomb potential of the muon and the nucleus "taken as one":

$$U^{(1)} = -\frac{(Z-1)e^2}{r} \tag{10}$$

The second term $U^{(2)}$ is the quadrupole potential term (the dipole moment of the muonic and nuclear "rings" is zero). In the spherical coordinates where the z-axis is the axis of symmetry of the muonic "ring", its part $U_\mu^{(2)}$ of the second term is

$$U_\mu^{(2)} = -e^2 R_\mu^2 \frac{3\cos^2\theta - 1}{4r^3} \tag{11}$$

In these expressions, r is the magnitude of the electron radius-vector and θ is its polar angle. The quadrupole potential energy of a charged ring is derived, e.g., in [21].

The expression for the quadrupole contribution of the nuclear "ring" is

$$U_{nucl}^{(2)} = Ze^2 R_{nucl}^2 \frac{3\cos^2\theta - 1}{4r^3} \tag{12}$$

Due to (9), the ratio $|U^{(2)}_\mu/U^{(2)}_{nucl}|$ has the following form:

$$\left|\frac{U_\mu^{(2)}}{U_{nucl}^{(2)}}\right| = \frac{R_\mu^2}{ZR_{nucl}^2} = \frac{M_{nucl}^2}{Zm_\mu^2} \gg 1 \tag{13}$$

For example, for helium $|U^{(2)}_\mu/U^{(2)}_{nucl}| = 622 >> 1$. For $Z > 2$, the ratio $|U^{(2)}_\mu/U^{(2)}_{nucl}|$ is even greater: due to the roughly linear dependence of M_{nucl} on Z, $|U^{(2)}_\mu/U^{(2)}_{nucl}|$ also depends roughly linearly on Z. Therefore, the effect of the nuclear "ring" on the quadrupole potential energy can be neglected for most practical purposes.

Thus, the effective potential energy of the electron takes the following form:

$$U_{eff} = -\frac{(Z-1)e^2}{r} - e^2 R_\mu^2 \frac{3\cos^2\theta - 1}{4r^3} \tag{14}$$

We can make a comparison of our expression for U_{eff} in (14) with the one for the potential energy U_E of a satellite in the oblate Earth's gravitational field (see, e.g., the book by Beletsky [22])

$$U_E = -\frac{GmM_E}{r} - GmM_E|I_2|R^2 \frac{3\cos^2\theta - 1}{2r^3} \tag{15}$$

In (15), m is the mass of the satellite, M_E is the mass of the Earth, R is the Earth's equatorial radius, and I_2 is a constant parameter describing the relative difference between the Earth's equatorial and polar diameters.

If we compare the following quantities in (15) with those in (14)

$$GmM_E = (Z-1)e^2, |I_2|R^2 = \frac{e^2R_\mu^2}{2GmM_E} = \frac{R_\mu^2}{2(Z-1)} \tag{16}$$

then the right-hand sides of (15) and (14) will become identical. This means that the Rydberg electron motion in muonic-electronic helium atoms or helium-like ions is mathematically identical to the motion of a satellite in the field of an oblate planet (such as the oblate Earth). The solution for such motion presented, e.g., in the book by Beletsky [22], shows that the satellite's elliptical orbit experiences two types of precession: the orbit precession in its own plane and the precession of the orbit plane around the axis parallel to the polar diameter of the Earth. The shape of the satellite orbit is unchanged under these two types of precession. Their frequencies are given by Eqs. (1.7.10) and (1.7.11) from Beletsky book [22].[3]

From the corresponding quantities in (16), we find the two precessions frequencies of the Rydberg electron orbit in muonic-electronic systems considered here. The precession of the orbit in its own plane has the frequency

$$\omega_{pip} = \frac{3}{8}\frac{Z-1}{Z^2}(1-5\cos^2 i)\left(\frac{m_\mu}{l_e+1/2}\right)^4\left(\frac{m_{er}}{m_{\mu r}}\right)^2\omega_K \tag{17}$$

where the Rydberg electron's Kepler frequency ω_K is given by (3), "pip" in the subscript index stands for "precession in plane", and i is the angle between the electron orbit plane and the plane of the muonic and nuclear "rings", called the inclination. To obtain (17), we used the relation between the semi-latus rectum p of the unperturbed elliptical orbit and the angular momentum M of the Rydberg electron:

$$p = \frac{M^2}{(Z-1)m_e e^2} = \frac{(l_e+1/2)^2\hbar^2}{(Z-1)m_e e^2} \tag{18}$$

where l_e is the electron's angular momentum quantum number.

The precession of the electron's orbital plane around the axis of symmetry of the muonic "ring" has the frequency

$$\omega_{pop} = \frac{3}{4}\frac{Z-1}{Z^2}\cos i\left(\frac{n_\mu}{l_e+1/2}\right)^4\left(\frac{m_{er}}{m_{\mu r}}\right)^2\omega_K \tag{19}$$

where "pop" in the subscript index stands for "precession of plane".

The above-mentioned situation is shown schematically in Figure 1. The bold dot represents the nucleus, the circle represents the muon ring, and the precessing elliptical orbit is of the electron.

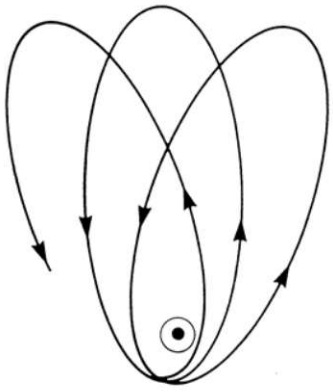

Fig. 1. The nucleus (bold dot), the muonic ring (circle), and the precessing orbit of the electron.

The motion of the Rydberg electron in muonic-electronic helium atoms or helium-like ions is also mathematically equivalent to the problem of a hydrogen Rydberg atom in an electric field with linear polarization $\mathbf{E}(t) = \mathbf{E}_0 \cos \omega_L t$ produced by a laser radiation of a high frequency, where the laser frequency ω_L is much greater than the Rydberg electron's Kepler frequency [24].

In all of the above-mentioned configurations the squared angular momentum M^2 is approximately conserved (besides the exact conservation of the projection M_z of the angular momentum onto the symmetry axis), which is the consequence of the fact that the shape of the elliptical orbit is unchanged under the precessions. Therefore, these configurations have a *hidden symmetry*, i.e., the *symmetry which is higher than the geometrical one* (in our case, the geometrical symmetry is the axial symmetry). Thus, the hidden symmetry of a muonic-electronic helium atom or helium-like ion in Rydberg states should be of *general physical interest*.

2.3. Conclusions

We studied muonic-electronic helium atoms or helium-like ions (we concentrated primarily on helium atoms), with both leptons in Rydberg states, and the muon in a circular Rydberg state. We used the appropriate here method of separating the rapid and slow subsystems, the subsystem "nucleus – muon" being rapid and the electron being slow.

We showed that the electron undergoes motion in a modified Coulomb potential, whose second term is the quadrupole interaction with the muonic "ring". Then we showed that the electron's effective potential energy mathematically coincides with the satellite's potential energy in an orbit about an oblate planet (for example, the oblate Earth). Using this, we concluded that the electron orbit experiences two different simultaneous precessions: the precession of the orbit in its own plane, and the precession of the orbital plane itself about the axis of symmetry of the muonic "ring". We analytically derived the expressions for the frequencies of both precessions.

The precessions mentioned above should be observed in spectral lines corresponding to the electron's radiative transitions as these two series of satellites. In the first one, the satellites would be separated (in the frequency scale) from the spectral line's unperturbed position by the frequency ω_{pip} (17) and its multiples. In the second one, the satellites would be separated (in the frequency scale) from the spectral line's unperturbed position by the frequency ω_{pop} (19) and its multiples.

We noted that the perturbation does not affect the shape of the electron's elliptical orbit, which manifests the (approximate) conservation of its squared angular momentum. This means that the configurations considered above possess a *hidden symmetry*. This result is *counterintuitive* and it presents a *general physical interest*. We also noted that the problem of the Rydberg electron motion in muonic-electronic helium atoms or helium-like ions mentioned above also mathematically coincides with the problem of a hydrogen Rydberg atom in an electric field with the linear polarization of a laser radiation of high frequency, as well as with the three-dimensional motion of a circumbinary planet about a binary star.

The results of this chapter and of our previous paper [2] complement each other. Therefore, these two works combined should improve a physical insight into Rydberg states of muonic-electronic helium atoms and helium-like ions.

CHAPTER 3. CLASSICAL DYNAMICS OF MUONIC-ELECTRONIC HELIUM AND HELIUM-LIKE IONS: THE ALLOWANCE FOR THE ECCENTRICITY OF THE MUON AND NUCLEUS ORBITS

3.1. Introduction

There are numerous applications of muonic atoms and molecules – see, e.g., [11-15] and references therein. This inspired the studies of systems μZe composed of a nucleus Z, an electron and a muon (see [1,2,16], Chapter 5 of [3] and Chapter 2 of the present review).

In particular, in Chapter 2 we studied Rydberg states of the muonic-electronic helium atom or helium-like ion, considering that the motion of the muon is much more rapid than the motion of the electron. Therefore, we employed

the analytical method of separating rapid and slow subsystems. It was shown that the electron motion occurs in a potential which is identical to that of a satellite about an oblate planet (for instance, a satellite about the Earth).

Then, in Chapter 2 we showed that the "unperturbed" electronic elliptical orbit undergoes two types of precession at the same time: the precession of the orbit of the electron in its own plane and the precession of the orbital plane of the electron around the axis of symmetry of the orbit of the muon. The shape of the elliptical orbit of the Rydberg electron, however, is unchanged. The conservation of the orbit's area means that the square of the angular momentum of the electron is conserved. Thus, the system possesses symmetry which is higher than geometrical: from the geometrical symmetry alone (which is axial), it only follows that the projection of the angular momentum on the axis of symmetry is conserved. This was a counterintuitive result which has a general physical interest.

In Chapter 2 we considered circular orbits of the muon and the nucleus. In this chapter we study a more general situation where the orbits of the muon and the nucleus are elliptical. We find how a relatively small eccentricity ε of their orbits changes the electronic motion. We find an additional term in the effective potential for the electronic motion. We demonstrate that in the particular case of the motion in the plane (where the orbits of the electron and the system "nucleus – muon" are in the same plane), there is an effect on the frequency of the precession of the orbit of the electron. We show that this contribution can have the same order of magnitude as the primary, eccentricity-independent contribution to the frequency of the precession.

3.2. New results

As in Chapter 2, here we study the configuration which consists of a nucleus of charge Z, a muon and an electron. Both leptons are in Rydberg states, which means that their principal quantum numbers are $n_\mu >> 1$ and $n_e >> 1$ ("μ" stands for the muon and "e" for the electron). The electron has a far greater distance from the nucleus than the muon because the two leptons have a large difference in their mass.

In this chapter we study the case of small-eccentricity orbits of the system "muon – nucleus". For a Coulomb potential

$$U = -\frac{\alpha}{r} \tag{20}$$

(where $\alpha = Ze^2$, and e is the elementary charge), the equation of the planar orbit is

$$\frac{p}{r} = 1 + \varepsilon\cos\varphi \tag{21}$$

Here

$$p = \frac{L^2}{m_r\alpha}, \varepsilon = \sqrt{1 + \frac{2EL^2}{m_r\alpha^2}} \tag{22}$$

where ε is the eccentricity of the orbit, (r, φ) are the polar coordinates, E is the energy, L is the angular momentum, and m_r is the reduced mass of the subsystem "particle – Coulomb center".

When the eccentricity is small ($\varepsilon << 1$), this gives

$$r = \frac{p}{1 + \varepsilon\cos\varphi} \approx p(1 - \varepsilon\cos\varphi) = r_0(1 - \varepsilon\cos\varphi) \tag{23}$$

where r_0 is the orbit radius for $\varepsilon = 0$. Because the situation with $\varepsilon = 0$ was studied in Chapter 2, the electron feels the rapid subsystem "nucleus – muon" as two rings of radii R_{nucl0} and $R_{\mu 0}$ charged uniformly, where $R_{\mu 0}/R_{nucl0} = m_{nucl}/m_\mu >> 1$. The potential for the electron then was

$$U_{eff}^{(0)} = -\frac{(Z-1)e^2}{r} - \frac{e^2(R_{\mu 0}^2 - ZR_{nucl0}^2)}{4r^3}(3\cos^2\theta - 1) \tag{24}$$

In the present situation $\varepsilon << 1$, R_{μ} and R_{nucl} have the dependence on time:

$$R_{\mu} = R_{\mu 0}(1 - \varepsilon\cos\Omega t), R_{nucl} = R_{nucl0}(1 - \varepsilon\cos\Omega t) \tag{25}$$

where

$$\Omega = \sqrt{\frac{Ze^2}{m_{\mu r}(R_{\mu 0} + R_{nucl0})^3}} \approx \sqrt{\frac{Ze^2}{m_{\mu r}R_{\mu 0}^3}} \tag{26}$$

is the revolution frequency of the system "nucleus – muon" about its center of mass, and

$$m_{\mu r} = \frac{m_{\mu}m_{nucl}}{m_{\mu} + m_{nucl}} \tag{27}$$

is the reduced mass of this system. Plugging (25) in (24), we receive this time-dependent "potential":

$$U(t) = U_{eff}^{(0)} + \frac{e^2(R_{\mu 0}^2 - ZR_{nucl0}^2)}{2r^3}(3\cos^2\theta - 1)\varepsilon\cos\Omega t \equiv U_{eff}^{(0)} + W(r, \cos\theta)\cos\Omega t \tag{28}$$

Now we employ the term $W(r, \cos\theta)\cos\Omega t$ in the method of effective potentials [24-28] with respect to the totally unperturbed Hamiltonian

$$H_0 = \frac{p^2}{2m_{er}} - \frac{(Z-1)e^2}{r} \tag{29}$$

where

$$m_{er} = \frac{m_e(m_{\mu} + m_{nucl})}{m_e + m_{\mu} + m_{nucl}} \tag{30}$$

is the reduced mass of the system "electron – the pair nucleus-muon". The helium atom ($Z = 2$) has $m_{er} = 0.9999$, therefore, in the case of any Z, m_{er} is practically equal to 1. Besides, since $R_{\mu 0}/R_{nucl0} >> 1$, we can omit R_{nucl0} from the potential.

The zeroth-order potential,

$$U_0 = \frac{1}{4\Omega^2}[W, [W, H_0]] = \frac{9\varepsilon^2 e^4 R_{\mu 0}^4(1 - 2\cos^2\theta + 5\cos^4\theta)}{16m_{er}\Omega^2 r^8} \tag{31}$$

where W is given in (28) and $[P, Q]$ are the Poisson brackets, is the time-independent term. Taking Ω from (26) and plugging it into (31), we get:

$$U_0 = \frac{9\varepsilon^2 m_{\mu r}e^2 R_{\mu 0}^4(1 - 2\cos^2\theta + 5\cos^4\theta)}{16m_{er}Zr^8} \tag{32}$$

Therefore, the full expression for the effective potential in this case is

$$\begin{aligned} U_{eff} &= U_{eff}^{(0)} + U_0 \\ &= -\frac{(Z-1)e^2}{r} - \frac{e^2R_{\mu 0}^2}{4r^3}(3\cos^2\theta - 1) \\ &+ \frac{9\varepsilon^2 m_{\mu r}e^2 R_{\mu 0}^4(1 - 2\cos^2\theta + 5\cos^4\theta)}{16m_{er}Zr^8} \end{aligned} \tag{33}$$

Next, we consider the electron orbits which are in the same plane as the muon – nucleus orbits, which means that $\theta = \pi/2$. This is stable equilibrium, as we can see from (33) differentiating it with respect to θ. Here, the resulting potential is a Coulomb potential with two additional $1/r^n$-perturbations (as before, we use the atomic units $e = m_e = \hbar = 1$):

$$U_{eff} = -\frac{Z-1}{r} + \frac{R_{\mu 0}^2}{4r^3} + \frac{9\varepsilon^2 m_{\mu r} R_{\mu 0}^4}{16 m_{er} Z r^8} \tag{34}$$

The derivation of the $1/r^n$-perturbation to the Kepler orbit is given, e.g., in [29] (the cases $n = 2$ and $n = 3$ were also considered in [17], Chapter 3, problem 3). In the case of the Coulomb potential $-\alpha/r$ with a perturbation by the potential $-\beta/r^{n+1}$, the orbit precesses with the perihelion advance

$$\delta\Phi = 2m\beta \frac{\partial}{\partial L}\left(\frac{1}{L} p^{1-n} \int_0^{\pi} (1 + \varepsilon_e \cos\varphi)^{n-1} d\varphi\right) \tag{35}$$

where m is the reduced mass of the system "particle – Coulomb center", L is the particle's angular momentum, ε_e is the orbit eccentricity, and $p = L^2/(m\alpha)$; in the case we are considering the particle is the electron. The precession frequency divided by the Kepler frequency is equal to the perihelion advance divided by 2π, so for the precession caused by the second term in (34), the frequency of the precession in the orbit plane divided by the Kepler frequency is

$$\frac{\omega_{pip}^{(1)}}{\omega_K} = -\frac{3}{4} m_{er}^2 (Z-1) S^2 \tag{36}$$

where

$$S = \frac{R_{\mu 0}}{L^2} \tag{37}$$

and "pip" in the subscript index in (36) stands for "precession in plane". We could come to an identical conclusion by using Eq. (1.7.10) from [22], where the potential is the oblate Earth gravitational potential and is mathematically the same as (32) (excluding the last term) with the quantities corresponding in this way:

$$GMm \Leftrightarrow (Z-1)e^2, I_2 R^2 \Leftrightarrow \frac{2\gamma}{e^2}, p \Leftrightarrow \frac{Z-1}{2|E|}, \gamma = \frac{e^2 R_{\mu 0}^2}{4(Z-1)} \tag{38}$$

(we employed the same approach in Chapter 2). Putting this correspondence into Eq. (1.7.10) from book [22] and using the above-mentioned assumption $\theta = \pi/2$, we get the same as (36) (again, $e = 1$ in the atomic units).

In Fig. 2, we have the plot of the ratio $|\omega_{pip}^{(1)}/\omega_K|$ depending on $R_{\mu 0}$ for the case of $L = 3$ and $Z = 2$. We see that at these values of $R_{\mu 0}$, the frequency $\omega_{pip}^{(1)}$ of the precession in the orbit plane stays small compared to the Kepler frequency ω_K of the electron, which serves as the validity condition for (36).

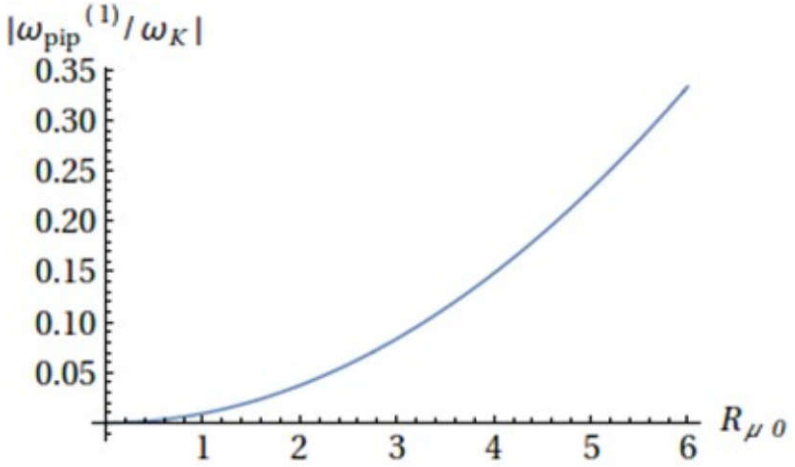

Fig. 2. Plot of the ratio $|\omega_{pip}^{(1)}/\omega_K|$ from (36) versus $R_{\mu 0}$ for $L = 3$ and $Z = 2$.

Applying (35) to the next perturbation term, which is the last term in (34), and which is the contribution to the potential from the small eccentricity of the orbits of the muon and the nucleus, we derive the additional term for the precession frequency (divided by the Kepler frequency):

$$\frac{\omega_{pip}^{(2)}}{\omega_K} = -\frac{63\varepsilon^2 m_{\mu r} m_{er}^6 (Z-1)^6 S^7 f(E_s)}{256Z}, f(E_s) = 429 - 495E_s + 135E_s^2 - 5E_s^3 \tag{39}$$

where

$$E_s = \frac{2|E|L^2}{m_{er}(Z-1)^2} \tag{40}$$

is the scaled dimensionless electron energy (taken by the absolute value). In the case of bounded electron motion, the orbit eccentricity is $\varepsilon_e = (1 - E_s)^{1/2}$ and $0 < E_s \leq 1$.

In Figure 3, we have $f(E_s)$ from (39). As E_s goes from zero to one, $f(E_s)$ monotonically diminishes from 429 down to 64.

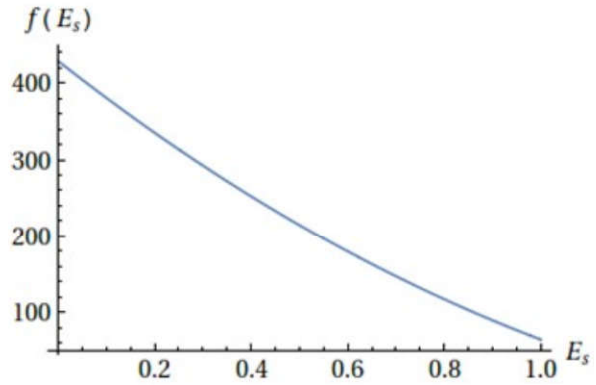

Fig. 3. Plot of the function $f(E_s)$ from (39), where E_s is the scaled electron energy defined in (40).

Fig. 4 presents the three-dimensional plot of $|\omega_{pip}^{(2)}/\omega_K|$ depending on $R_{\mu 0}$ and ε for $E_s << 1$ (the case of a large electron orbit eccentricity $(1 - \varepsilon_e) << 1$), $L = 3$, and $Z = 2$ (which means that $m_{\mu r} = 200.4$). We see that at these values of $R_{\mu 0}$ and ε, the next-order contribution to the frequency of the precession $\omega_{pip}^{(2)}$ stays sufficiently less than the electron Kepler frequency ω_K, which is the validity condition for the analytical result for $\omega_{pip}^{(2)}/\omega_K$ from (39).

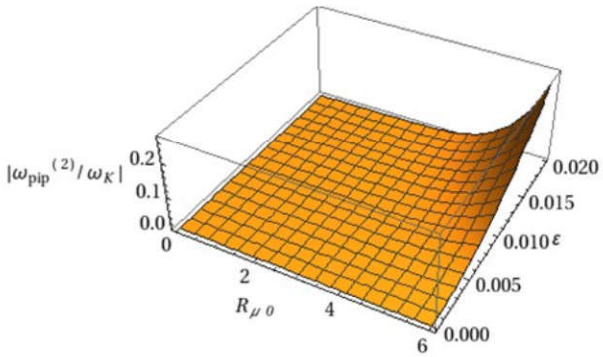

Fig. 4. Plot of the ratio $|\omega_{pip}^{(2)}/\omega_K|$ from (39) depending on $R_{\mu 0}$ and ε for $E_s << 1$, $L = 3$, and $Z = 2$.

The ratio $\omega_{pip}^{(2)}/\omega_{pip}^{(1)}$ (which we name K_{21}) of the next-order term of the precession frequency (39) to the primary term (36) is:

$$K_{21} = \frac{21\varepsilon^2 m_{\mu r} m_{er}^4 (Z-1)^5 S^5 f(E_s)}{64Z} \tag{41}$$

Figure 5 presents K_{21} depending on $S = R_{\mu 0}/L^2$ and E_s (see (40)) for the case of $Z = 2$ and $\varepsilon = 0.02$.

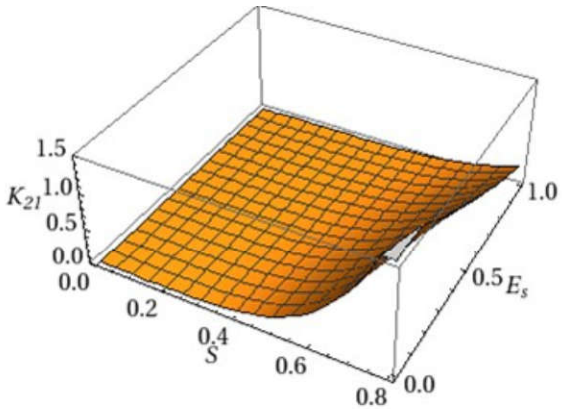

Fig. 5. Plot of the ratio K_{21} of next-order term of the precession frequency (38) to the primary term (36) depending on $S = R_{\mu 0}/L^2$ and E_s (see (40)) for $Z = 2$ and $\varepsilon = 0.02$.

Figure 6 presents K_{21} depending on S and Z for $\varepsilon = 0.02$ and $E_s << 1$.

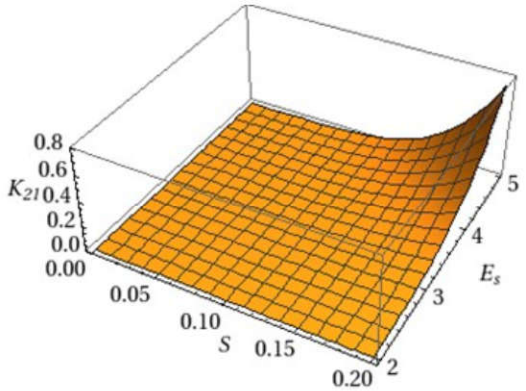

Fig. 6. Plot of K_{21} depending on S and Z for $\varepsilon = 0.02$ and $E_s << 1$.

Figure 7 presents K_{21} depending on $R_{\mu 0}$ and ε for the case of $Z = 2$, $L = 3$, and $E_s << 1$.

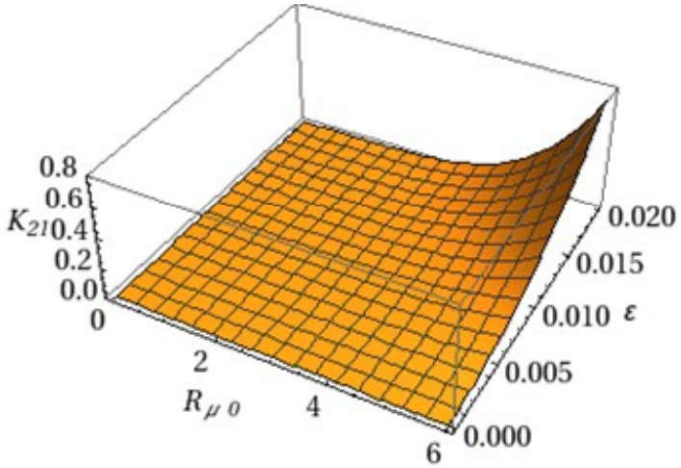

Fig. 7. Plot of K_{21} depending on $R_{\mu 0}$ and ε for the case of $Z = 2$, $L = 3$, and $E_s << 1$.

From Figs. 5 – 7 we see that within the ranges of the parameters where the validity conditions for both primary and additional contributions to the precession frequency are satisfied, $\omega_{pip}^{(2)}$, the additional contribution because of a low eccentricity of the muon orbit (and of the nucleus orbit) can be of the same order of magnitude as the primary contribution $\omega_{pip}^{(1)}$.

3.3. Conclusions

We studied the case where the muon and nucleus orbits in the "nucleus-muon-electron" system are elliptical, which is a more general situation compared to Chapter 2, where the muon and nucleus orbits under consideration were circular. In the situation of a relatively small eccentricity of the orbits of the muon and the nucleus, we obtained an additional, eccentricity-dependent contribution to the effective potential for the electron. We showed analytically that in the planar case (where the orbit of the electron is in the same plane as the orbits of the muon and the nucleus), it yields an additional eccentricity-dependent term of the precession frequency of the orbit of the electron. We demonstrated that this additional term can reach the same order of magnitude as the primary term, which does not depend on the eccentricity of the orbit. Therefore, these results in this chapter have not only qualitative, but also quantitative importance.

CHAPTER 4. CIRCULAR RYDBERG STATES OF HELIUM ATOMS OR HELIUM-LIKE IONS IN A HIGH-FREQUENCY LASER FIELD

4.1. Introduction

In [30,24,31] studies of a hydrogenic atoms/ions in a laser field of high-frequency were carried out. To give more details, in [24,31] the focus was at classically-described Rydberg states. In [24,31], by "high-frequency" it was meant that frequency ω of the laser is much greater than the Kepler frequency $\omega_K = m_e e^4/(n^3\hbar^3)$ of the atom: $\omega >> \omega_K$. (m_e is the electron mass, e is the electron charge, and $n >> 1$ is the electronic principal quantum number.) In this model, the laser field can be considered the fast subsystem and the Rydberg atom – the slow subsystem, which allows an analytical solution. Particularly, in paper [24] the authors generalized the method of effective potentials previously developed by Kapitza [27,28].

In [30,24,31] it was shown that this problem reveals interesting physics. With the laser field of linear or circular polarization, the system possesses axial symmetry, which means that the squared angular momentum M^2 is not conserved (only M_z, the projection of the angular momentum on the axis of symmetry is conserved). However, in [30,24,31] it was demonstrated that in this case M^2 is approximately conserved, so that this system possesses approximate algebraic symmetry, which is higher than the geometrical symmetry.

Besides, in the cases of linear or circular polarization of the laser field, the system has celestial analogies. Particularly, in the case of linear polarization, the electron motion is analogous to the satellite motion in the gravitational field of an oblate planet: it undergoes two precessions – the orbit precession within its own plane and the precession of the orbital plane itself. In the case of circular polarization, the electron motion is the same as the satellite motion in the gravitational field of a (nonexistent) prolate planet: it undergoes the same two precessions.

We devote this chapter to the study of a helium atom or a helium-like ion whose one of the two electrons is in a Rydberg state, while the system is under a laser field of high frequency. To obtain results, we use the method of effective potentials [24,25], also given in book [26].

Then we considered circular Rydberg states of the electron (see the first footnote to Chapter 2, Section 1). We demonstrate that there is precession of the orbital plane of the Rydberg electron caused by the laser field of high frequency. We find the frequency of the precession analytically and show that it is different than the one for a hydrogenic atom/ion. This precession would manifest itself in the radiation spectrum as satellites separated from the spectral line at the Kepler frequency by the multiples of the frequency of the precession.

Another result that we found in this situation is that the laser field of high frequency induces a red shift of the electron energy. We find this shift of energy analytically and analyze how it depends on the system parameters.

4.2. New results

We consider a He atom or a He-like ion in a laser field of high frequency. The inner electron of the atom or ion is in state 1s and the outer electron is highly-excited. The quasinucleus, which is comprised of the nucleus of charge Z and

a spherically-symmetric charge distribution given by the inner electron in state 1s, has the following potential (see, e.g, [32]):

$$\Phi(r) = \frac{Z-1}{r} + (Z\mu + \frac{1}{r})e^{-2Z\mu r} \tag{42}$$

where $\mu = M_n m_e/(M_n + m_e)$ is the reduced mass of the "nucleus – electron" (M_n is the mass of the nucleus and m_e of the electron) and r is the distance between the symmetry center and the outer electron. Atomic units $\hbar = e = m_e = 1$ are used here. The atom is submerged into a high-frequency laser field which has frequency ω and amplitude F. It is appropriate to use a classical or semi-classical analysis for Rydberg electrons.

4.2.1. Linearly-polarized laser field

For linear polarization, the semi-classical Hamiltonian for the outer (Rydberg) electron is

$$H = H_0 + zF\cos\omega t, H_0 = \frac{1}{2\mu_1}(p_r^2 + \frac{p_\theta^2}{r^2} + \frac{p_\varphi^2}{r^2\sin^2\theta}) - \Phi(r) \tag{43}$$

where $\mu_1 = m_e(M_n + m_e)/(M_n + 2m_e)$ is the reduced mass of the system "nucleus Z with the inner electron – outer electron", the z-axis is in the same direction as the laser field **F**, (r, θ, φ) are the electron spherical coordinates, F is the laser field strength and ω is its frequency. Both μ and μ_1 are close to unity: physically, they are in the range from 0.999864 for helium ($Z = 2$) to 0.999998 for He-like oganesson ($Z = 118$). The configurations in a field of high frequency (far exceeding the largest frequency of the unperturbed system) can be treated using the method of effective potentials [24-28]. The result of this procedure is an additional time-independent term in the Hamiltonian H_0. The effective potential of the zeroth-order,

$$U_0 = \frac{1}{4\omega^2}[V,[V,H_0]] = \frac{F^2}{4\mu_1\omega^2} \tag{44}$$

where $V = zF$ and the square brackets denote the Poisson brackets, is a shift of energy without coordinate dependence and therefore it has no effect on the system dynamics. The effective potential of the first order is the first that affects the system dynamics:

$$U_1 = \frac{1}{4\omega^4}[[V,H_0],[[V,H_0],H_0]] =$$
$$= -\frac{F^2(Z\mu)^3}{8\mu_1^2\omega^4x^3}((Z-1)(1+3\cos2\theta) + ((1+2x)(1+2x^2) + (3+6x+6x^2+4x^3)\cos2\theta)e^{-2x}) \tag{45}$$

where

$$x = \mu Z r \tag{46}$$

The electron effective potential energy then is

$$U_{eff} = U + U_0 + U_1 \tag{47}$$

with U being the unperturbed energy.

In [24], where the subject of study was a hydrogen Rydberg atom in a laser field of high frequency with linear polarization, the effective potential energy was shown to have the following form:

$$U_{eff}(r,\theta) = -\frac{e^2}{r} - \frac{\gamma}{r^3}(3\cos^2\theta - 1), \gamma = \frac{e^4F^2}{4m_e^2\omega^4} \tag{48}$$

where θ is the polar angle in the spherical coordinates, i.e., the angle between the electron radius-vector **r** and the z-axis directed along the laser field amplitude **F**. This effective potential energy has mathematical equivalence to the satellite potential energy in the gravitational field of the oblate Earth (see, e.g., [32]), and it bears the following

feature: in the general case of the elliptical unperturbed orbit, the latter undergoes two simultaneous precessions. The first is the precession of the elliptical orbit in its own plane, and the second is the precession of the orbital plane itself about the vector **F**. The frequencies of both have the same order of magnitude and they are much less than the Kepler frequency of the electron.

In our case the general form of the effective potential energy is more complex. Therefore, we consider a particular situation where the unperturbed electron orbit is circular. In this situation the orbital precession in the plane does not apply, and only the precession of the plane of the orbit is considered.

Thus, we consider the case r = const, so the only dynamic variable is the angle θ. In such a case, we can bring the potential energy to the form (48) with an extra term independent of θ, as shown below. Defining

$$f(x) = (1 + 2x)(1 + 2x^2), g(x) = 3 + 6x + 6x^2 + 4x^3 \tag{49}$$

we transform (45) into the following expression:

$$U_1 = -\frac{F^2(Z\mu)^3(Z-1)}{4\mu_1^2\omega^4 x^3}((3\cos^2\theta - 1)(1 + g(x)\frac{e^{-2x}}{3(Z-1)}) + \frac{3f(x) - g(x)}{2}\frac{e^{-2x}}{3(Z-1)}) \tag{50}$$

The total energy of the electron is therefore

$$U_{eff} \approx -\frac{Z-1}{r} + \Delta U_1(r) + \Delta U(r, \cos\theta) \tag{51}$$

where the second term is the shift of energy compared to the unperturbed energy, and the third term is the one that causes the precession.

From (50) and (48), the term

$$g(x)\frac{e^{-2x}}{3(Z-1)} \tag{52}$$

is a relative correction to the frequency of the precession of the plane of the orbit, and the quantity

$$\frac{3f(x) - g(x)}{2}\frac{e^{-2x}}{3(Z-1)} = 4x^3\frac{e^{-2x}}{3(Z-1)} \tag{53}$$

corresponds to a shift of energy. Incorporating the factor at the start of (50), we obtain the energy shift:

$$\delta E = -\frac{F^2(Z\mu)^3}{3\mu_1^2\omega^4}e^{-2x} \tag{54}$$

In circular orbits, the outer electron has the energy $E = -(Z-1)/(2r)$, and, taking the quantity defined in (46), the energy shift can be given the following form:

$$\delta E = -\frac{F^2(Z\mu)^3}{3\mu_1^2\omega^4}e^{\frac{\mu Z(Z-1)}{E}} \tag{55}$$

Figure 8 presents the energy shift depending on the unperturbed energy of the electron for $Z = 4$, $F = 1$, $\omega = 100$. The Kepler frequency of the electron at such energies,

$$\omega_K = \frac{1}{Z-1}\sqrt{\frac{8|E|^3}{\mu_1}} \tag{56}$$

is in fact much less than the frequency of the laser field.

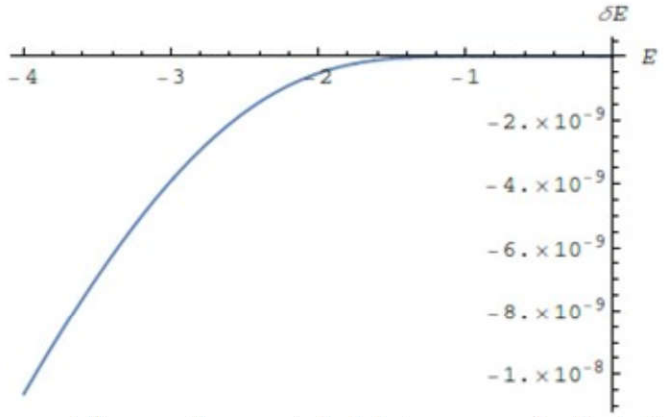

Fig. 8. The energy shift versus the unperturbed electron energy for $Z = 4$, $F = 1$, $\omega = 100$.

We see that the energy shift vanishes when the unperturbed energy is zero, and it has the asymptotic limit $-F^2(Z\mu)^3/(3\mu_1^2\omega^4)$ as the absolute value of the unperturbed energy increases (see Fig. 9).

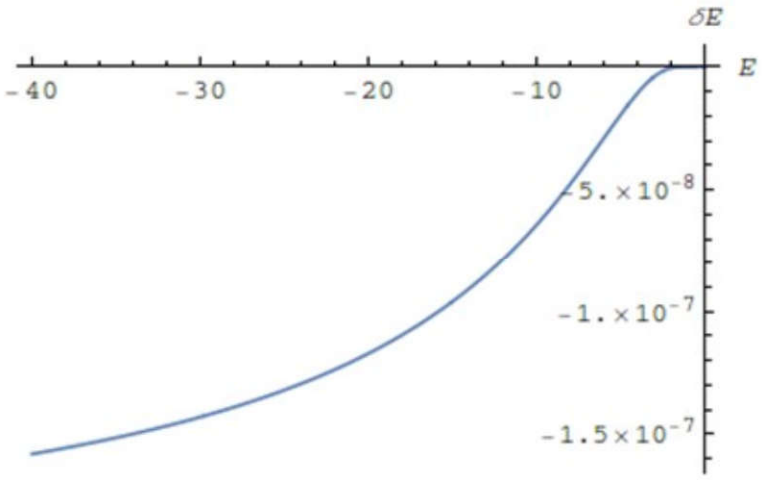

Fig. 9. The energy shift versus the unperturbed electron energy E for $Z = 4$, $F = 1$, $\omega = 100$ for large negative values of E.

In Figure 10 we present the shift of energy depending on the charge Z of the nucleus at $F = 1$ and $\omega = 100$ for the two selected values of the unperturbed energy: $E = -2$ (blue, solid line) and $E = -5$ (red, dashed line). It has a minimum at the point $Z_m \approx (1 + (1 + 24|E|)^{1/2})/4$ (using the approximate values $\mu = \mu_1 = 1$). The non-monotonic dependence of the shift of energy on Z is *counterintuitive*.

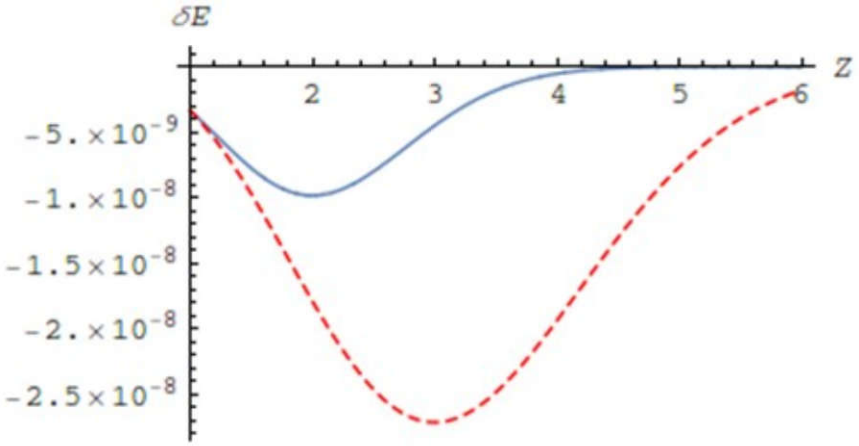

Fig. 10. The energy shift versus the nuclear charge Z for $E = -2$ (blue, solid line) and $E = -5$ (red, dashed line) for $F = 1$, $\omega = 100$.

In Figure 11 we present a plot of the shift of energy depending on both the charge of the nucleus and the unperturbed energy for the values $F = 1$ and $\omega = 100$. We see that the minimum of the shift in relation to the nuclear charge in fact moves to greater values of Z as the absolute value of the unperturbed energy increases.

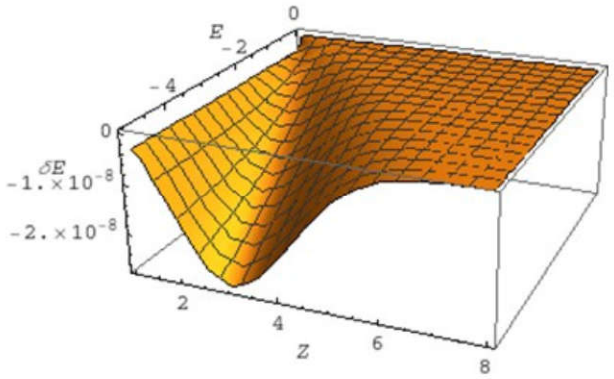

Fig. 11. The dependence of the energy shift on Z and E for $F = 1$, $\omega = 100$.

The motion described by the effective potential energy

$$U_{eff} = -\frac{(Z-1)e^2}{r} - \frac{(Z-1)\gamma}{r^3}(3\cos^2\theta - 1) \tag{57}$$

has mathematical equivalence to the satellite motion in the gravitational field of the oblate Earth, whose effective potential in the latter case is (see, e.g., [32])

$$V_E = -\frac{GM_E m}{r} - \frac{GM_E m|I_2|R^2}{2r^3}(3\cos^2\theta - 1) \tag{58}$$

Here M_E is the mass of the Earth, m is the mass of the satellite, R is the Earth equatorial radius, and I_2 is a constant parameter describing the relative difference between the equatorial and polar diameters of the Earth. The ratio of the precession frequency Ω of the plane of the satellite to the Kepler frequency ω_K is [22]:

$$\frac{\Omega}{\omega_{E,K}} = \frac{3|I_2|}{2}\left(\frac{R}{p}\right)^2 \cos i \tag{59}$$

where

$$\omega_{E,K} = \sqrt{\frac{G(M_E + m)}{A_s^3}} \tag{60}$$

is the satellite Kepler frequency, m is the mass of the satellite, and A_s is the major semi-axis of its unperturbed elliptical orbit. In (59), i is the angle between the orbit plane of the satellite, also called the *inclination*, and the equatorial plane of the Earth. p is the semi-latus rectum of the unperturbed orbit.

If we bring into the correspondence the following quantities in (58) with those in (57)

$$GM_E m = (Z-1)e^2, |I_2|R^2 = \frac{2\gamma}{e^2} \tag{61}$$

then the energy expression from (58) would become identical to (57). By substituting $|I_2|R^2 = 2\gamma/e^2$ in (59), we get the corresponding expression for the ratio of the frequencies for our case:

$$\frac{\Omega}{\omega_K}|_0 = \frac{3\gamma}{e^2 p^2}\cos i \tag{62}$$

where the Kepler frequency ω_K is given by (56) and the subscript "0" refers to the unperturbed case.

In circular orbits,

$$p = r = \frac{Z-1}{2|E|} \tag{63}$$

so that the ratio for the unperturbed case in (62) becomes

$$\frac{\Omega}{\omega_K}|_0 = \frac{12\gamma|E|^2}{(Z-1)^2}\cos i \tag{64}$$

where in our case the quantity γ is (see (50))

$$\gamma = \frac{F^2}{4\mu_1^2\omega^4} \tag{65}$$

The dependence of x from (64) on the unperturbed energy in the case of circular orbits is

$$x = \mu Z r = \frac{\mu Z(Z-1)}{2|E|} \tag{66}$$

In (51), $\Delta U_1(r)$ is a relatively small shift of the electron energy. The motion beyond the plane of the unperturbed circular orbit is described by the truncated $U_{eff,\,tr}$ (see (50), (51)):

$$U_{eff,tr} = -\frac{Z-1}{r} - \frac{(Z-1)\gamma}{r^3}(1 + g(x)\frac{e^{-2x}}{3(Z-1)})(3\cos^2\theta - 1) \tag{67}$$

where $g(x)$ is from (49), r is from (63) and x from (66). Therefore, the frequency of the precession divided by the electron Kepler frequency is

$$\frac{\Omega}{\omega_K} = \frac{3\gamma}{r^2}(1 + g(x)\frac{e^{-2x}}{3(Z-1)})\cos i = \frac{12\gamma|E|^2}{(Z-1)^2}(1 + g(x)\frac{e^{-2x}}{3(Z-1)})\cos i \tag{68}$$

and the relative correction to the precession frequency is

$$\frac{\Delta\Omega}{\Omega} = g(x)\frac{e^{-2x}}{3(Z-1)} \tag{69}$$

with $g(x)$ from (49) and $x(E)$ from (66).

In Figure 12 we show the relative correction to the frequency of the precession of the orbital plane of the Rydberg electron depending on the energy of the electron for a few values of Z.

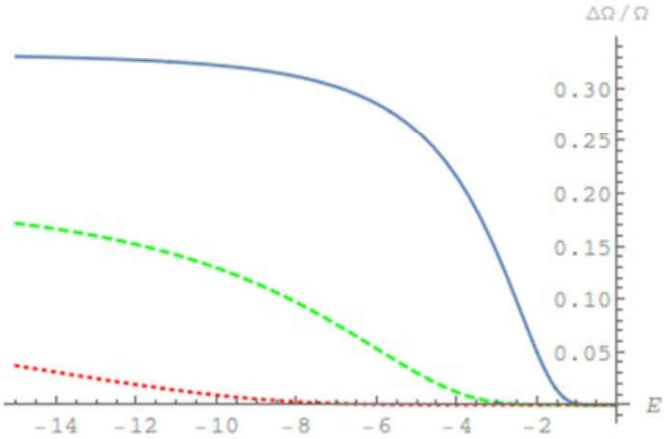

Fig. 12. Dependence of the relative correction to the precession frequency of the orbital plane of the Rydberg electron on the electron energy for $Z = 4$ (blue solid curve), $Z = 6$ (green dashed curve), and $Z = 9$ (red dotted curve).

The relative correction to the precession frequency $\Delta\Omega/\Omega$ has an asymptotic limit of $1/(Z-1)$ at large negative values of the electron energy.

4.2.2. Circularly-polarized laser field

In this section we consider the case of the laser field of the amplitude F and frequency ω with circular polarization, the polarization field being orthogonal to the z-axis. The time variation of the laser field is

$$\mathbf{F}= F(\mathbf{e}_x \cos\omega t + \mathbf{e}_y \sin\omega t) \tag{70}$$

where $\mathbf{e}_x$ and $\mathbf{e}_y$ are the orts of the x- and y-axes (orthogonal to the z-axis). The semi-classical Hamiltonian of the outer electron here has the form

$$H = H_0 + xF\cos\omega t + yF\sin\omega t \tag{71}$$

where H_0 is given in (43). Denoting

$$V = xF = Fr\sin\theta\cos\varphi, W = yF = Fr\sin\theta\sin\varphi \tag{72}$$

where (r, θ, φ) are the spherical coordinates, and applying the method of effective potentials [24-26], we obtain the effective potential of the zeroth order

$$U_0 = \frac{1}{4\omega^2}([V,[V,H_0]] + [W,[W,H_0]]) = \frac{F^2}{2\mu_1\omega^2} \tag{73}$$

and of the first order

$$\begin{aligned} U_1 &= \frac{1}{4\omega^4}([[V,H_0],[[V,H_0],H_0]] + [[W,H_0],[[W,H_0],H_0]]) + \frac{-1}{2\omega^3}[[V,H_0],[W,H_0]] = \\ &= \frac{F^2(Z\mu)^3}{8\mu_1^2\omega^4x^3}((Z-1)(1+3\cos2\theta) + ((1+2x+2x^2-4x^3) + (3+6x+6x^2+4x^3)\cos2\theta)e^{-2x}) \end{aligned} \tag{74}$$

with x given in (46). Repeating the derivation from the linear-polarization case, we present U_1 in the same form as in (50):

$$U_1 = \frac{F^2(Z\mu)^3(Z-1)}{4\mu_1^2\omega^4x^3}((3\cos^2\theta-1)(1+g(x)\frac{e^{-2x}}{3(Z-1)}) + \frac{3f_1(x)-g(x)}{2}\frac{e^{-2x}}{3(Z-1)}) \tag{75}$$

The differences from (50) are the initial sign and another function $f_1(x)$:

$$f_1(x) = 1 + 2x + 2x^2 - 4x^3 \tag{76}$$

From (75) we find that the shift of energy caused by the circularly-polarized laser field is

$$\delta E = -\frac{2F^2(Z\mu)^3}{3\mu_1^2\omega^4}e^{-2x} \tag{77}$$

which is twice as large as the one caused by the linearly-polarized laser field. The relative correction to the frequency of the precession of the orbital plane in the circular-polarization case is found to be identical to the linear-polarization case (given in (52) and (69)).

4.3. Conclusions

We considered a helium atom or a helium-like ion with one of the two electrons in a Rydberg state, the atom being placed into a laser field of high frequency. We used the generalized method of effective potentials from [24-26] to obtain the analytical results.

Then we considered circular Rydberg states. It was found that there are two main effects of the laser field. The first one is the precession of the orbital plane of the Rydberg electron. We found the frequency of the precession and demonstrated that it is different from the one in the case of a hydrogen atom/hydrogen-like ion. In the radiation

spectrum this precession should manifest itself as satellites separated from the Kepler frequency spectral line by multiples of the frequency of the precession. The second effect is the red shift of the energy of the Rydberg electron because of the laser field; we found the analytical expression for this shift. We studied how it depends on the system parameters. We found that the shift monotonically increases by absolute value when the Rydberg electron unperturbed binding energy increases. Besides, we demonstrated that the shift depends non-monotonically on the nuclear charge Z: this dependence has a maximum. The non-monotonic dependence of the energy shift caused by the laser field on the charge of the nucleus is *counterintuitive*.

Finally we would like to mention that for the interaction between atoms and a laser field of high frequency, the method of effective potentials [27,28,25], which we used in the present chapter, is more advantageous than the method given by Kramers [33] and Henneberger [34], and after that used by Gavrila *et al*. in the treatment of hydrogen atoms [35,36]. The latter method essentially consists of switching to the frame which oscillates with an electron in the laser field and then time-averaging of the corresponding time-dependent perturbation. Nevertheless, first, this method applied to hydrogen atoms in the laser field of high frequency, as in the paper by Gavrila [35], fails to detect the hidden (algebraic) symmetry of the system, which was revealed in papers [30,24] using the method of effective potentials; thus, the method of Kramers–Henneberger does not have the physical insight in comparison with the method of effective potentials. Second, the method of effective potentials is carried out analytically to the arbitrary order with respect to the laser field [25,26], but this feature is apparently not present in the method of Kramers–Henneberger.

CHAPTER 5. CIRCULAR RYDBERG STATES OF LITHIUM ATOMS OR LITHIUM-LIKE IONS IN A HIGH-FREQUENCY LASER FIELD

5.1. Introduction

In Chapter 4 and [37], we considered a helium atom or a helium-like ion in a laser field of high frequency. In this chapter we study a lithium atom or a lithium-like ion in a laser field of high frequency. The atom/ion under consideration has two inner electrons in the state 1s, and the third, outer, electron is in a highly excited (Rydberg) state. The potential Φ of a configuration of a nucleus of charge Z and two inner electrons in state 1s is [32,38]

$$\Phi = \frac{Z-2}{r} + 2((Z-\frac{5}{16})\mu + \frac{1}{r})e^{-2(Z-\frac{5}{16})\mu r} \tag{78}$$

where $\mu = M_n m_e/(M_n + m_e)$ is the reduced mass of the system "nucleus Z – electron" (M_n is the nucleus mass and m_e is the electron mass) and r is the distance between the electron and the center of the atom. We use atomic units: $\hbar = e = m_e = 1$. The atom is in a high-frequency laser field of frequency ω and amplitude F. Rydberg electrons can be treated classically or semi-classically.

5.2. New results

5.2.1. Linearly-polarized laser field

First, we consider the linear polarization of the laser field. The outer electron has the following Hamiltonian:

$$H = H_0 + zF\cos\omega t, H_0 = \frac{1}{2\mu_1}(p_r^2 + \frac{p_\theta^2}{r^2} + \frac{p_\varphi^2}{r^2\sin^2\theta}) - \Phi(r) \tag{79}$$

where $\mu_1 = m_e(M_n + 2m_e)/(M_n + 3m_e)$ is the reduced mass of the system "nucleus Z with the two inner electrons – outer electron", the z-axis is collinear with the laser field $\mathbf{F}$, (r, θ, φ) are the electron spherical coordinates. μ and μ_1 are very close to unity: they are in the range from 0.999922 for lithium ($Z = 3$) to 0.999998 for Li-like oganesson ($Z = 118$). To study systems in a high-frequency field, when the field frequency is much larger than the highest frequency of the unperturbed system, it is appropriate to use the method of effective potentials [24-28]. Applying this method yields a time-independent term added to the Hamiltonian H_0. The effective potential of the zeroth order,

$$U_0 = \frac{1}{4\omega^2}[V,[V,H_0]] = \frac{F^2}{4\mu_1\omega^2} \tag{80}$$

where $V = zF$ and $[P, Q]$ are the Poisson brackets, is a coordinate-independent shift of energy and thus it does not affect the dynamics of the system. The effect on the system dynamics is given by the effective potential of the first order:

$$U_1 = \frac{1}{4\omega^4}[[V,H_0],[[V,H_0],H_0]] =$$
$$= -\frac{F^2((Z-\frac{5}{16})\mu)^3(Z-2)}{4\mu_1^2\omega^4x^3}\left(\frac{8x^3}{3(Z-2)}e^{-2x} + (3\cos^2\theta - 1)\left(1+\frac{2g(x)}{3(Z-2)}e^{-2x}\right)\right) \tag{81}$$

where x is similar notation to that in (46) and used in [37]:

$$x = \mu(Z-\frac{5}{16})r \tag{82}$$

and

$$g(x) = 3 + 6x + 6x^2 + 4x^3 \tag{83}$$

For $x << 1$, (81) becomes

$$U_1 \approx \frac{F^2Z}{4\mu_1^2\omega^4}\frac{1-3\cos^2\theta}{r^3} \tag{84}$$

Its only difference from the corresponding effective potential of the first order, obtained in [24] for a hydrogen Rydberg atom in a high-frequency laser field with linear polarization, is the factor Z. As given in [24], this type of effective potential is a mathematical analogue of the satellite potential energy which orbits around the oblate Earth [22].

The most important physical detail of this kind of effective potential is that the corresponding system has a *higher than geometrical symmetry*. It reveals itself as the conservation of the squared angular momentum M^2, while from the geometrical (axial) symmetry, only the conservation of the projection M_z of the angular momentum on the laser field direction follows. For the configuration studied in the present chapter, allowing for finite values of $x = \mu(Z - 5/16)r$ *breaks this algebraic symmetry* and reduces it to the geometrical (axial) symmetry.

As given in Chapter 4 and in [37] and references therein, the perturbation (81) modifies the unperturbed Coulomb potential and shows the following physical behavior: for the general case of an elliptic orbit, the orbit undergoes two precessions: one is the precession of the elliptic orbit in its own plane, and the other one is the precession of the plane of the orbit itself about the vector **F**. The frequencies of both precessions have the same order of magnitude, and they are much smaller than the electron's Kepler frequency. As in Chapter 4 and [37], we consider a circular unperturbed orbit of the outer electron. In this situation the first kind of precession (of the elliptic orbit in its plane) loses its meaning and we consider only the second precession (of the orbital plane).

The potential (81) resembles the potential for the helium-like case in (50), which we reproduce here for comparison:

$$U_1 = -\frac{F^2(Z\mu)^3(Z-1)}{4\mu_1^2\omega^4x^3}\left(\frac{4x^3}{3(Z-1)}e^{-2x} + (3\cos^2\theta - 1)\left(1+\frac{g(x)}{3(Z-1)}e^{-2x}\right)\right) \tag{85}$$

Thus, the quantity

$$\frac{\Delta\Omega}{\Omega} = \frac{2g(x)}{3(Z-2)}e^{-2x} \tag{86}$$

is a relative correction to the precession frequency of the orbit plane, and

$$\delta E = -\frac{F^2((Z-\frac{5}{16})\mu)^3(Z-2)}{4\mu_1^2\omega^4 x^3}\frac{8x^3}{3(Z-2)}e^{-2x} = -\frac{2F^2((Z-\frac{5}{16})\mu)^3}{3\mu_1^2\omega^4}e^{-2x} \tag{87}$$

is a shift of energy. For a circular orbit, the outer electron energy is $E = -(Z-2)/(2r)$ and, taking (82), we obtain the expression for x depending on the unperturbed energy:

$$x(E) = \mu(Z-\frac{5}{16})r = -\frac{\mu(Z-\frac{5}{16})(Z-2)}{2E} \tag{88}$$

and then we give the energy shift the following form:

$$\delta E = -\frac{2F^2((Z-\frac{5}{16})\mu)^3}{3\mu_1^2\omega^4}e^{\frac{\mu(Z-\frac{5}{16})(Z-2)}{E}} \tag{89}$$

Figure 13 presents the shift of energy depending on the unperturbed electron energy for the selected values of $Z = 4$, 6 and 9 in the laser field with $F = 1$ and $\omega = 80$.

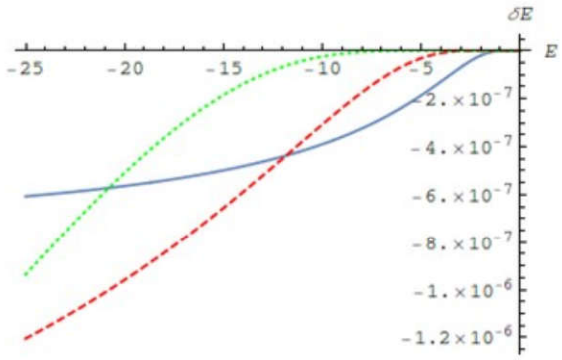

Fig. 13. The energy shift versus the unperturbed electron energy for $Z = 4$ (blue, solid curve), $Z = 6$ (red, dashed curve) and $Z = 9$ (green, dotted curve) for $F = 1$, $\omega = 80$.

It is seen that the energy shift vanished at the zero unperturbed energy and has the limit $-2F^2((Z-5/16)\mu)^3/(3\mu_1{}^2\omega^4)$ as the unperturbed energy increases by the absolute value. Calculating the ratio of the shift of energy in our case to that in the helium-like case given by (55), which becomes

$$\frac{\delta E}{\delta E_{He}} = 2(1-\frac{5}{16Z})^3 e^{-\frac{(21Z-10)\mu}{16E}} \tag{90}$$

we see that for negative E and $Z \geq 2$, this ratio always exceeds unity, so for the given value of the outer electron energy, the shift is always greater by the absolute value in the lithium-like case than in the helium-like case.

Figure 14 presents the shift depending on the charge Z of the nucleus. Looking at the similarity of it with Figure 10 in Chapter 4, we notice that it is similar, and the lithium-like case has a greater shift.

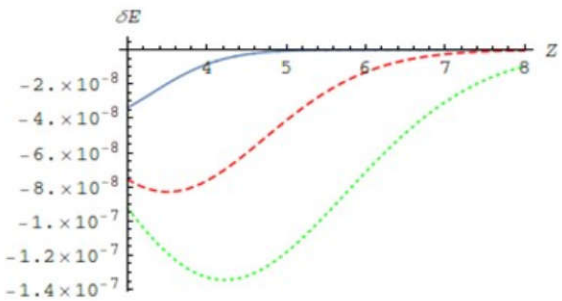

Fig. 14. The energy shift versus the nuclear charge Z for $E = -2$ (blue, solid curve), $E = -5$ (red, dashed curve) and $E = -8$ (green, dotted curve) for $F = 1$, $\omega = 100$.

It is seen that with the growth of Z, the absolute value of the energy shift first increases, then attains a maximum value, and then decreases. The non-monotonic dependence of the shift on the charge of the nucleus is *counterintuitive*.

Figure 15 presents the ratio of the lithium-like shift to the helium-like one given by (90) as a function of the electron energy, for the charge of the nucleus $Z = 4$.

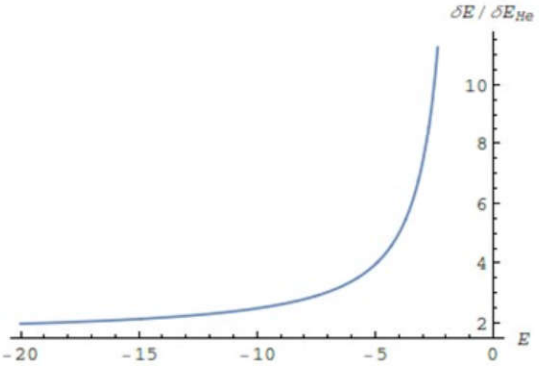

Fig. 15. The ratio of the energy shift in the Li-like case to the one in the He-like case, depending on the energy of the electron, for $Z = 4$.

Figure 16 shows the ratio of the lithium-like energy shift to the helium-like one given by (90) as a function of the charge of the nucleus, for the value of electron energy $E = -10$.

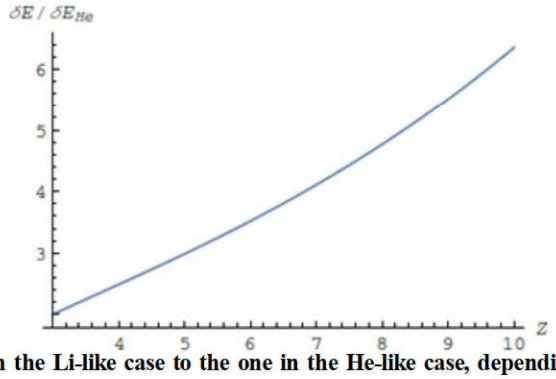

Fig. 16. The ratio of the energy shift in the Li-like case to the one in the He-like case, depending on the nuclear charge, for $E = -10$.

The relative correction to the frequency of the precession of the plane is (86). Taking the outer electron energy for circular orbits, $E = -(Z-2)/(2r)$, and (82), the relative correction $\delta\Omega$ as a function of E and Z is

$$\delta\Omega = \frac{\Delta\Omega}{\Omega} = \frac{2g(x(E))}{3(Z-2)} e^{-2x(E)} \tag{91}$$

with $g(x)$ in (83) and $x(E)$ in (88).

Figure 17 shows the relative correction as a function of the electron energy for selected values of Z.

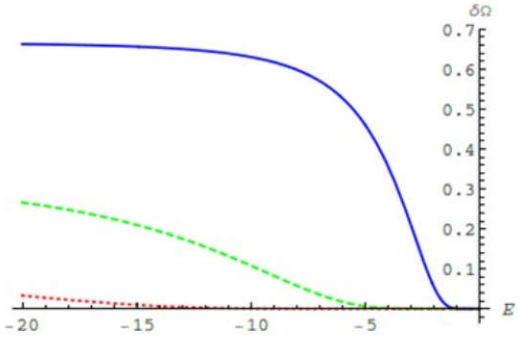

Fig. 17. The relative correction to the precession frequency of the orbital plane of the Rydberg electron versus the electron energy for $Z = 5$ (blue solid curve), $Z = 8$ (green dashed curve), and $Z = 12$ (red dotted curve).

We observe that for $Z = 5$, the relative correction is approximately 2/3 in the large part of the energy range. The correction $\delta\Omega = \Delta\Omega/\Omega$ goes to the limit of $2/(Z-2)$ at large negative energy values.

To compare the relative correction $\delta\Omega$ in this (lithium-like) case to the relative correction in the helium-like case, we calculate their ratio (the correction for the present case is in (91) and the correction for the helium-like case is in (69) and (66) in Chapter 4):

$$\delta\Omega_{He} = \frac{g(x_{He}(E))}{3(Z-1)} e^{-2x_{He}(E)}, x_{He}(E) = -\frac{\mu Z(Z-1)}{2E} \tag{92}$$

The ratio of the two relative corrections is therefore

$$\frac{\delta\Omega}{\delta\Omega_{He}} = 2\frac{Z-1}{Z-2}\frac{g(x(E))}{g(x_{He}(E))} e^{-\frac{(21Z-10)\mu}{16E}} \tag{93}$$

with $g(x)$ in (83), $x(E)$ in (88), and $x_{He}(E)$ in (92). For the case of $Z \geq 2$ and $E < 0$, (93) is strictly larger than 1, so $\delta\Omega$ is always larger here than in the helium-like case, given the energy of the outer electron and the charge of the nucleus.

We need to underline that in the radiation spectrum, this precession would cause satellites with the distances from the spectral line at the Kepler frequency being equal to multiples of the frequency of the precession. Thus, our result with the more exact expression for the precession frequency is important for the analysis of experiments.

5.2.2. Circularly-polarized laser field

Here we analyze the situation with the laser field having circular polarization, as well as the amplitude F and frequency ω, when the field of the polarization is orthogonal to the z-axis. This can be put into the expression

$$\mathbf{F} = F(\mathbf{e_x}\cos\omega t + \mathbf{e_y}\sin\omega t) \tag{94}$$

In this expression $\mathbf{e_x}$ and $\mathbf{e_y}$ are the orts of the x- and y-axes (orthogonal to the z-axis). The outer electron Hamiltonian is therefore

$$H = H_0 + xF\cos\omega t + yF\sin\omega t \tag{95}$$

where H_0 is given in (79). Denoting

$$V = xF = Fr\sin\theta\cos\varphi, W = yF = Fr\sin\theta\sin\varphi \tag{96}$$

where (r, θ, φ) are the spherical coordinates, and applying the method of effective potentials [24-28], we obtain the following effective potential of the zeroth order:

$$U_0 = \frac{1}{4\omega^2}([V,[V,H_0]] + [W,[W,H_0]]) = \frac{F^2}{2\mu_1\omega^2} \tag{97}$$

and of the first order:

$$U_1 = \frac{1}{4\omega^4}([[V,H_0],[[V,H_0],H_0]] + [[W,H_0],[[W,H_0],H_0]]) + \frac{-1}{2\omega^3}[[V,H_0],[W,H_0]] =$$
$$= \frac{F^2((Z-\frac{5}{16})\mu)^3(Z-2)}{4\mu_1^2\omega^4x^3}(-\frac{16x^3}{3(Z-2)}e^{-2x} + (3\cos^2\theta - 1)(1 + \frac{2g(x)}{3(Z-2)}e^{-2x})) \tag{98}$$

From (98) and (85), the latter representing the linear-polarization case, it is seen that the shift of energy is two times greater than that of the linear-polarization case, and the precession frequency correction is equal to that of the linear-polarization case.

5.3. Conclusions

We analyzed a lithium atom or a lithium-like ion in a laser field of high frequency. We obtained the effective potential and demonstrated that if the outer electron's distance from the nucleus is relatively small, the effective potential differs only by a factor Z from the effective potential obtained in [24] for a hydrogen Rydberg atom in a high-frequency laser field with linear polarization. We observed that in this case the effective potential is identical to the satellite potential in the field of oblate Earth. We noted that the systems having this kind of effective potential possess *higher than geometrical symmetry* characterized by the conservation of the squared angular momentum (in spite of the geometrical symmetry being axial rather than spherical).

In the configuration analyzed in this chapter, after allowing for finite values of r, we had the case of *broken algebraic symmetry*. The symmetry was reduced to geometrical.

For circular Rydberg states we found a more exact value of the precession frequency of the Rydberg electron orbital plane. This precession would cause satellites, whose distance from the spectral line at the Kepler frequency equals multiples of the precession frequency. Thus, our result on the more exact value of the frequency of the precession is important for the comparative analysis of experiments.

We also found the red shift of the highly-excited electron energy due to the laser field of high frequency. We demonstrated that as the unperturbed binding energy of the Rydberg electron increases, the shift monotonically increases by the absolute value. Nonetheless, the dependence of the shift on the charge of the nucleus turned out to be non-monotonic. This is a *counterintuitive* result.

CHAPTER 6. CONCLUSIONS OF THE REVIEW

In this work we studied muonic systems and atoms in a high-frequency laser field. Specifically, in Chapter 2, we studied muonic-electronic helium atoms or helium-like ions (primarily focusing on helium atoms), in which both leptons are in Rydberg states, with the muon in a circular Rydberg state. We used the method of separation of rapid and slow subsystems, showing that the subsystem "nucleus – muon" can be treated as rapid, while the electron as slow. We showed that the Rydberg electron effective potential energy is mathematically identical to the satellite potential energy in the gravitational field of an oblate planet (e.g., the oblate Earth). Using this, we showed that the electron's unperturbed orbit experiences two different simultaneous precessions: one of them is the orbit precession in its plane, and the other is the precession of the orbital plane around the axis of the muonic "ring". We found analytically the frequencies of both precessions. These precessions should manifest in spectral lines corresponding to the radiative transitions of the electron as the two series of satellites as follows. In the first series, the satellites would be separated (in the frequency scale) from the unperturbed position of the spectral line by the frequency ω_{pip} ("pip" stands for "precession in plane") and its multiples; in the second series, by the frequency ω_{pop} ("pop" stands for "precession of plane") and its multiples. We emphasized that the perturbation does not change the shape of the elliptical orbit of the Rydberg electron, which manifests the (approximate) conservation of the squared angular momentum of the Rydberg electron. This shows that the above-mentioned physical systems possess a *hidden symmetry*, which is a *counterintuitive* result of *general physical interest*. We noted that the above problem of the Rydberg electron motion in muonic-electronic helium atoms or helium-like ions is also mathematically identical to a hydrogen Rydberg atom in a linearly-polarized electric field of a laser radiation of high frequency, and also to the three-dimensional motion of a circumbinary planet around a binary star.

In Chapter 3, we studied a more general situation than in Chapter 2, namely where the muon and nucleus have elliptical orbits. For the case of the eccentricity of the muon and nucleus orbits being relatively small, we found an additional eccentricity-dependent term in the effective potential for the electron motion. We showed analytically that in the special case where the orbit of the electron is in the plane of the muon and nucleus orbits, it gives an additional contribution to the precession frequency of the electron orbit. We showed that this additional eccentricity-dependent contribution can reach the same order of magnitude as the primary, eccentricity-independent contribution to the precession frequency.

In Chapter 4, we studied a helium atom or a helium-like ion with one of its two electrons in a Rydberg state, with

the system submerged into a laser field of high frequency. To solve the problem analytically, we used the generalized method of effective potentials. We considered circular Rydberg states. We saw two main effects of the high-frequency laser field. The first effect is the precession of the Rydberg electron's orbital plane. We found an analytical expression for the precession frequency and showed that it is different from the one in the case of a hydrogenic atom/ion. In the radiation spectrum, this precession would manifest as satellites separated from the spectral line at the Kepler frequency by multiples of the precession frequency. The second effect is a red shift of the energy of the Rydberg electron caused by the high-frequency laser field. We found an analytical expression for this shift. We studied its dependence on the system parameters. We found that the shift monotonically increases by absolute value as the unperturbed binding energy of the Rydberg electron increases. Besides, we found that the shift depends non-monotonically on the nuclear charge Z: this dependence has a maximum. The non-monotonic dependence of the energy shift caused by the laser field on the nuclear charge is a *counterintuitive* result.

In Chapter 5, we studied a lithium atom or a lithium-like ion, with one of its three electrons being in a Rydberg state, with the system submerged into a laser field of high frequency. To solve the problem analytically, we employed the generalized method of effective potentials. We demonstrated that for a relatively small distance between the outer electron and the nucleus, the system possesses *higher than geometrical symmetry*. For an arbitrary distance between the outer electron and the nucleus, we had the case of the *broken algebraic symmetry* reduced to the geometrical (axial) symmetry. We performed the analysis of the following two outcomes for circular Rydberg states. One of the outcomes is the precession of the orbit plane of the highly excited electron – we calculated analytically the frequency of this precession. It causes the following changes of the radiation spectrum: the appearance of satellites at the distances from the unperturbed frequency of the spectral line equal to multiples of the precession frequency. The other outcome is a shift of energy of the Rydberg electron. The dependence of this shift on the charge of the nucleus was shown to be a non-monotonic function.

Notes

1. We note that circular Rydberg states (CRS) of atoms were studied extensively [4-7] theoretically and experimentally for the following reasons. First, it was because CRS have long radiative lifetimes and strongly anisotropic collision cross sections, so that they facilitate experiments on inhibited spontaneous emission and cold Rydberg gases [8,9]. Second, classical CRS are counterparts to fundamentally important quantal coherent states. Third, in the quantal method using the $1/n$-expansion (n being the principal quantum number), the primary term corresponds to the classical description (see, e.g. paper [10] and references therein). (See Part I, Chapter 1 [3].)
2. In paper [2] the authors treated this system as a modified "rigid rotator" consisting of the electron, the nucleus, and the ring, over which the muon charge is uniformly distributed, all distances within the system being fixed. In other words, it was assumed that as the muon rapidly revolves in a circular orbit about the axis connecting the nucleus and electron, this axis slowly rotates, thus adiabatically following a relatively slow electronic motion. This assumption is valid only for a limited time.
3. We note that Eqs. (1.7.10) and (1.7.11) from Beletsky book [22] are also present in [23] where the three-dimensional motion of a circumbinary planet about a binary star is considered. [23] shows that this problem is also mathematically equivalent to the satellite motion about an oblate planet.

References

[1] N. Kryukov and E. Oks, Can. J. Phys. **91** (2013) 715.

[2] N. Kryukov and E. Oks, Can. J. Phys. **92** (2014) 1405.

[3] N. Kryukov and E. Oks, Dynamics **2** (2022) 73.

[4] E. Lee, D. Farrelly, and T. Uzer, Optics Express **1** (1997) 221.

[5] T.C. Germann, D.R. Herschbach, M. Dunn, and D.K. Watson, Phys. Rev. Lett. **74** (1995) 658.

[6] C.H. Cheng, C.Y. Lee, and T.F. Gallagher, Phys. Rev. Lett. **73** (1994) 3078.

[7] L. Chen, M. Cheret, F. Roussel, and G. Spiess, J. Phys. B **26** (1993) L437.

[8] S.K. Dutta, D. Feldbaum, A. Walz-Flannigan, J.R. Guest, and G. Raithel, Phys. Rev. Lett. **86** (2001) 3993.

[9] R.G. Hulet, E.S. Hilfer, and D. Kleppner, Phys. Rev. Lett. **55** (1985) 2137.

[10] V.M. Vainberg, V.S. Popov, and A.V. Sergeev, Sov. Phys. JETP **71** (1990) 470.

[11] L.I. Ponomarev, Contemp. Phys. **31** (1990) 219.

[12] K. Nagamine, Hyperfine Interactions **138** (2001) 5.

[13] K. Nagamine and L.I. Ponomarev, Nucl. Phys. A **721** (2003) C863.

[14] C. Chelkowsky, A.D. Bandrauk, and P.B. Corkum, Laser Physics **14** (2004) 473.

[15] J. Guffin, G. Nixon, D. Javorsek II, S. Colafrancesco, and E. Fischbach, Phys. Rev. D **66** (2002) 123508.

[16] E. Oks, Can. J. Phys. **98** (2020) 857.

[17] L.D. Landau and E.M. Lifshitz, *Mechanics* (Pergamon, Oxford, 1965).

[18] L.D. Landau and E.M. Lifshitz, *Quantum Mechanics* (Pergamon, Oxford, 1965).

[19] P.J. Redmond, Phys. Rev. **133** (1964) B1352.

[20] N. Kryukov and E. Oks, Phys. Rev. A **85** (2012) 054503.

[21] http://www.physics.princeton.edu/~mcdonald/examples/ph501set1.pdf (problem 5).

[22] V.V. Beletsky, *Essays on the Motion of Celestial Bodies* (Birkhäuser/Springer, Basel, 2001), Sect. 1.7.

[23] E. Oks, New Astronomy **74** (2020) 101301.

[24] B.B. Nadezhdin and E. Oks, Sov. Tech. Phys. Letters **12** (1986) 512.

[25] B.B. Nadezhdin, in *Radiatsionnye i Relativistskie Effekty v Atomakh i Ionakh* (Radiative and Relativistic Effects in Atoms and Ions), (Scientific Council of the USSR Academy of Sciences on Spectroscopy, Moscow, 1986), p. 222, in Russian.

[26] E. Oks, *Analytical Advances in Quantum and Celestial Mechanics: Separating Rapid and Slow Subsystems* (IOP Publishing, Bristol, UK, 2019).

[27] P.L. Kapitza, Sov. Phys. JETP **21** (1951) 588.

[28] P.L. Kapitza, Uspekhi Fiz. Nauk **44** (1951) 7.

[29] https://pages.uoregon.edu/dbelitz/teaching/lecture_notes/Mechanics%20(DB)/611_2_Lecture_Notes.pdf, p. 95.

[30] V.P. Gavrilenko, E. Oks, and A.V. Radchik, Opt. Spectrosc. **59** (1985) 411.

[31] E. Oks, J.E. Davis, and T.J. Uzer, J. Phys. B **33** (2000) 207.

[32] B.B. Nadezhdin and E.A. Oks, Opt. Spectrosc. **68** (1990) 12.

[33] H.A. Kramers, Collected Scientific Papers. Amsterdam: NorthHolland, Amsterdam, 1956, p. 262.

[34] W.C. Henneberger, Phys. Rev. Lett. **21** (1968) 838.

[35] M. Pont and M. Gavrila, Phys. Lett. A **123** (1987) 469.

[36] M. Pont, M.J. Offerhaus and M. Gavrila, Z. Phys. D - Atoms, Molecules and Clusters **9** (1988) 297.

[37] N. Kryukov and E. Oks, Open Physics **19** (2021) 11.

[38] H.A. Bethe and E.E. Salpeter, *Quantum Mechanics of One- and Two-Electron Atoms* (Springer, Berlin, 1957).